Parsons−Lee and Monte Carlo Study of Soft Repulsive Nematogens

A. Cuetos,† B. Martínez-Haya,* and S. Lago

Departamento de Ciencias Ambientales, Universidad Pablo de Olavide, 41013 Seville, Spain

L. F. Rull

Departamento de Física Atómica, Molecular y Nuclear, Area de Física Teórica, Universidad de Sevilla, Apdo. 1065, 41080 Seville, Spain

Received: April 8, 2005; In Final Form: May 19, 2005

A general approach based on the Parsons−Lee theory for soft repulsive molecular fluids is employed to investigate the nematogenic behavior of prolate thermotropic liquid crystals over a broad temperature range. The theory is solved for the particular case of the Kihara soft repulsive spherocylinder model, which is mapped into an effective hard core interaction with a temperature-dependent molecular diameter, expected to resemble the average size and shape of the soft molecules at a given temperature. The reduction of the effective molecular diameter with temperature in the Kihara soft repulsive fluid implies implicitly an increase of the elongation of the molecule and induces the stabilization of the nematic phase at smaller effective packing fractions, contrary to what is found for other fluid models. The rationalization of this effect in terms of excluded volume steric arguments is corroborated by the good general agreement between the Parsons−Lee approach and Monte Carlo simulations for the equation of state of the fluid in the vicinity of the isotropic−nematic transition.

I. Introduction

The phenomenology related to the spontaneous appearance of long-range orientational order in molecular fluids is of fundamental and practical importance. Nematic phases have provided a fertile framework for the understanding of liquid crystal behavior and for the discrimination of the relevance of the intermolecular interactions and the steric and many-body effects present in the fluid. Different theoretical approaches to the nematogenic behavior of molecular fluids have been proposed.[1] The seminal second-order virial theories of Onsager[2] and Maier and Saupe[3,4] were followed by more refined and higher-order treatments with the common theme of the minimization of the free energy of the fluid as a functional of the molecular orientational distribution function. Among these, the so-called Parsons−Lee (P−L) decoupling approximation proposed by different authors[5−8] and employed in the present work has constituted one of the most fruitful procedures, yielding progressively more general and accurate studies of nematic and other liquid crystal phases in pure and binary fluid systems.[9−13]

The hard spherocylinder (HSC) fluid constitutes a benchmark rigid model for the study of mesogenic behavior. Extensive theoretical and computational investigations based on this model fluid[14−22] have demonstrated that alone the hard core repulsive interaction that characterizes the HSC potential explains correctly the progression of isotropic, nematic, smectic, and solid phases typical of prolate liquid crystals. This is for instance in contrast to the hard ellipsoid fluid, another model of historical importance, in which layered smectic phases are not formed.[23] It may therefore be concluded that the spherocylinder geometry (a cylinder capped by hemispheres, see Figure 1) captures effectively the main steric excluded volume effects that drive the appearance of liquid crystalline order. One of the simplest variants of the HSC model arises from the substitution of the hard core of the potential by a soft repulsive interaction. Such a modification not only allows for a more realistic treatment of the compressibility of the fluid, but in addition, it introduces in a natural way a magnitude as crucial as temperature, which does not have an explicit role in the HSC fluid. A further advantage of the soft interaction models is that their implementation in molecular dynamics computations is straightforward, provided that the potential and its first derivative are continuous in the whole configurational domain of dynamic relevance. Soft repulsive models have played a relevant role in the development of perturbation theories for fluids of prolate molecules[24−29] and have been employed to study a variety of thermodynamic and structural properties of molecular fluids, with particular success for the description of colloidal systems.[17−19,30]

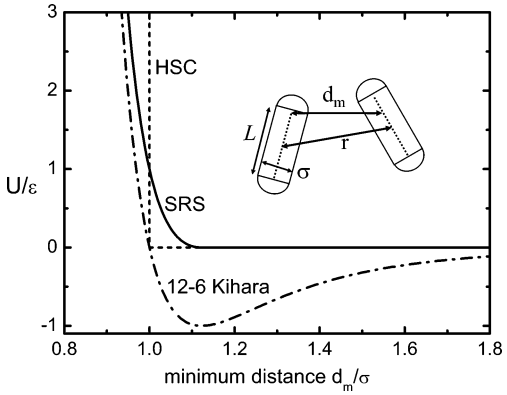

Figure 1. Pair interaction energy as a function of the minimum distance between the molecular cores, d_m, for the Kihara SRS potential, the 12−6 Kihara potential, and the HSC potential.

In the present work, we consider the Kihara soft repulsive spherocylinder (SRS) fluid, built from the truncation of the well-

* Corresponding author. E-mail: bmarhay@upo.es.

† Present address: Soft Condensed Matter, Debye Institute, Utrecht University, 3584CC Utrecht, The Netherlands.

10.1021/jp051834c CCC: $30.25
Published on Web 06/24/2005

known 12−6 Kihara potential.[31,32] The choice of this particular model is based on its recognized relevance in benchmark theoretical methods as a reference system with direct links to both the HSC and Kihara fluids.[27−29] The liquid crystal phase diagram of the Kihara SRS fluid has been however scarcely investigated. Aoki and Akiyama[33] employed molecular dynamics to study the stability of the nematic and smectic phases for SRS molecules of moderate elongation ($L^* = L/\sigma < 3$). More recently, Earl et al.[34] carried out a detailed study of the mesogenic behavior of the SRS fluid of elongation $L^* = 4$. Martınez-Haya and co-workers[21] extended the investigations to $L^* = 5$ and showed that at sufficiently high temperatures the isotropic−nematic−smectic phase diagram is displaced to greater densities with respect to that of the HSC fluid, whereas at low temperatures the reverse is true.[13,34] These latter results suggested that the effective size of the molecules and hence the steric effects responsible for the liquid crystal transitions depend crucially on the interpenetration of the particles into the repulsive wall of the pair interaction potential, which is enhanced as the temperature of the fluid increases. The dependence of the effective molecular size on temperature, packing fraction, or other environmental parameters affecting pair interactions is an old idea that stems from the work of Onsager[2] and has been extended by different authors more recently.[14,17,19,35] In the present work, we intend to explore this aspect in further detail by investigating the behavior of the SRS fluid in the vicinity of the isotropic−nematic transition over a broad range of temperatures.

In the following sections of the paper, a Parsons−Lee approach to the equation of state and isotropic−nematic phase coexistence of the SRS fluid is presented. The solution of the theory is based on the representation of the SRS interaction by an effective HSC potential with a molecular diameter only dependent on temperature. The results of this theoretical approximation are evaluated by means of a detailed comparison to Monte Carlo (MC) simulations in the isobaric−isothermal NPT ensemble. Overall, it is shown that the crude representation of the soft repulsive potential by an effective hard wall provides a reasonable qualitative and even quantitative picture of the steric effects involved in the equilibrium properties of the fluid in the isotropic and nematic phases.

II. Methodology

A. Interaction Model. Figure 1 compares the SRS interaction potential with the HSC and 12−6 Kihara potentials and serves also to illustrate that the SRS interaction potential is built from the truncation (at the well minimum) and shift of the 12−6 Kihara potential. In this way, a continuous and derivable (the first derivative is also continuous) purely repulsive interaction potential energy functional is obtained:

$$U_{\mathrm{SRS}}(r,\Omega) = \begin{cases} 4\epsilon[(\sigma/d_{\mathrm{m}})^{12} - (\sigma/d_{\mathrm{m}})^{6} + {}^{1}/_{4}] & d_{\mathrm{m}} \le d_{\mathrm{min}} \\ 0 & d_{\mathrm{m}} > d_{\mathrm{min}} \end{cases} \tag{1}$$

Here, σ is a parameter directly related to the diameter of the cylindrical body of the molecule, whereas ϵ modulates the intensity of the interaction. Note that in the 12−6 Kihara potential $d_{\mathrm{min}} = \sqrt[6]{2}\sigma$ and ϵ are the location and depth of the attractive well minimum, respectively. The molecular core in the Kihara fluids is usually characterized by the elongation $L^* = L/\sigma$, where L is the length of the central cylinder. In the present work, we consider the SRS fluid with $L^* = 5$. The function $d_{\mathrm{m}}(r,\Omega)$, characteristic of the spherocylinder core potentials,[31] represents the minimum distance between the central rodlike cores of the pair of interacting molecules (see Figure 1). This function can be efficiently computed numerically[36] and depends on the distance between the center of mass of the pair of molecules, r, and on their relative orientation as described by three independent angles (represented in short form by Ω).

Figure 1 shows, on one hand, the longer range of the SRS interaction in comparison to the HSC fluid, and on the other hand, the shift of the repulsive wall of the SRS potential with respect to the Kihara potential, which must be taken into account when comparing the behavior of these model fluids, can be appreciated.

B. Parsons−Lee Approach for the HSC Fluid. The present application of the P−L formalism is based on the formulation of McGrother and co-workers for the HSC fluid,[15] so that only the relevant or specific details concerning our work are discussed here. The method relies on the use of the Parsons−Lee decoupling approximation, with a correspondence between the HSC fluid and the hard sphere (HS) fluid with equal molecular volumes. In this way, the following expression for the free energy of the HSC fluid is obtained:

$$\frac{\beta F}{N} = \frac{\beta F_{\mathrm{iso}}^{\mathrm{id}}}{N} + \int f(\omega)\ln(4\pi f(\omega))\,\mathrm{d}\omega + \frac{1}{8v_{\mathrm{m}}}\frac{\beta F_{\mathrm{HS}}^{\mathrm{ex}}}{N}\int v_{\mathrm{exc}}(\gamma)\, f(\omega)\, f(\omega')\,\mathrm{d}\omega\,\mathrm{d}\omega' \tag{2}$$

where $\beta = (k_{\mathrm{B}}T)^{-1}$ (k_{B} is the Boltzmann constant), $v_{\mathrm{m}} = \pi\sigma^3/6 + \pi\sigma^2 L/4$ is the physical volume of the HSC particles, and $v_{\mathrm{exc}}(\gamma) = 4\pi\sigma^3/3 + 2\pi\sigma^2 L + 2\sigma L^2|\sin\gamma|$ represents the volume of physical space mutually excluded by a pair of particles describing an angle of $\gamma \equiv \gamma(\omega,\omega')$ between their principal axis.

The free energy of the isotropic ideal gas of rigid symmetric linear molecules is given by

$$\frac{\beta F_{\mathrm{iso}}^{\mathrm{id}}}{N} = \ln(\rho\Lambda^3\xi^2/4\pi) - 1 \tag{3}$$

where $\rho = N/V$ is the number density and $\Lambda = h/\sqrt{2\pi m k_{\mathrm{B}}T}$ and $\xi = h/\sqrt{2\pi I k_{\mathrm{B}}T}$ arise from the translational and rotational contributions to the partition function, respectively, with m and I being the mass and moment of inertia of the molecules and h being the Planck constant. In addition, within the present approximation, $F_{\mathrm{HS}}^{\mathrm{ex}}$ in eq 2 corresponds to the Carnahan−Starling excess free energy of the HS reference fluid:[15]

$$\frac{\beta F_{\mathrm{HS}}^{\mathrm{ex}}}{N} = \frac{4\eta - 3\eta^2}{(1-\eta)^2} \tag{4}$$

where $\eta = \rho v_{\mathrm{m}}$ denotes the packing fraction.

The function $f(\omega)$ plays a central role in the present approach and denotes the single-particle orientation distribution on the spherical coordinates $\omega \equiv (\phi,\cos\theta)$ with respect to a fixed "laboratory" frame, here defined by the nematic director of the fluid. Whereas in the isotropic phase $f(\omega) = (4\pi)^{-1}$ and the computation of the free energy is straightforward, in the nematic phase, the determination of $f(\omega)$ requires a numerical minimization procedure.[14,15] We have followed the ideas of different authors[37−40] and have performed a formal minimization of the free energy with respect to variations in $f(\omega)$. In this way, the

following expression is obtained:

$$\ln(4\pi f(\omega)) = \lambda + 1 - \frac{2b}{\pi v_m}\frac{4\eta - 3\eta^2}{(1-\eta)^2}\int |\sin\gamma| f(\omega')\, d\omega' \quad (5)$$

where λ is a Lagrange multiplier and $b = (\pi/4)\sigma L^2$. For molecules with cylindrical symmetry, as in the present case, the orientation distribution function does not depend on the azimuthal angle, that is, $f(\omega) = (2\pi)^{-1} f(\theta)$, and the formalism proceeds by expanding $f(\theta)$ in terms of the even Legendre polynomials:[38]

$$f(\theta) = \sum_{n=0}^{\infty} a_{2n} P_{2n}(\cos\theta) \quad (6)$$

A similar expansion is performed for $|\sin\gamma|$, which is analytical:[37]

$$|\sin\gamma| = \frac{\pi}{4} - \sum_{n=1}^{\infty} d_{2n} P_{2n}(\cos\gamma) \quad (7)$$

$$d_{2n} = \frac{\pi(4n+1)(2n-3)!!(2n-1)!!}{2^{2n+2} n!(n+1)!}$$

Taking into account the orthogonality of the Legendre polynomials, the combination of eqs 5−7 leads to the final formal equation for $f(\theta)$:

$$f(\theta) = K \exp\left[\frac{-4b}{v_m}\frac{4\eta - 3\eta^2}{(1-\eta)^2}\sum_{n=0}^{\infty}\frac{2}{4n+1} a_{2n} d_{2n} P_{2n}(\cos\theta)\right] \quad (8)$$

where K is a normalization factor. At this point, a self-consistent iteration is performed in order to compute the coefficients a_{2n} (and hence $f(\theta)$) at a given packing fraction. To ensure full convergence,[40] in the present work, the necessary truncation of the expansion of eqs 6−8 had to be performed at values as large as $n = 10$.

Once $f(\theta)$ is converged, the expression of the free energy (eq 2) allows for the calculation of the different thermodynamic quantities. The pressure and the chemical potential are in particular obtained from the usual relations:

$$p = -\left(\frac{\partial F}{\partial V}\right)_{T,N}, \quad \mu = \left(\frac{\partial F}{\partial N}\right)_{T,V} \quad (9)$$

The above expressions were also used to determine the states of coexistence at the isotropic−nematic transition. In this case, the iterative process is combined with the solution of the mechanical and chemical equilibrium conditions, $p_I = p_N$ and $\mu_I = \mu_N$, employing the Newton−Raphson method. We finally note that the nematic order parameter, $S_2 = \langle P_2(\cos\theta)\rangle$, relevant to the present work, can be obtained directly by performing the indicated average of the second Legendre polynomial over the $f(\theta)$ probability distribution.

C. Mapping of the SRS Fluid into the HSC Fluid. The Parsons−Lee procedure described so far applies to a fluid of hard spherocylinder particles with a well-defined diameter, σ, and length, L. To be able to implement the methodology for the investigation of the soft repulsive SRS fluid, we will assume that this latter fluid can be described by a HSC model of same length, L, but with an effective diameter, σ_{ef}, accounting for the interpenetration of the compressible molecular core of the SRS molecules. To describe the dependence of σ_{ef} on temperature, we have employed the following expression proposed by Boublik[27] as an extension of the Barker−Henderson theory:[24]

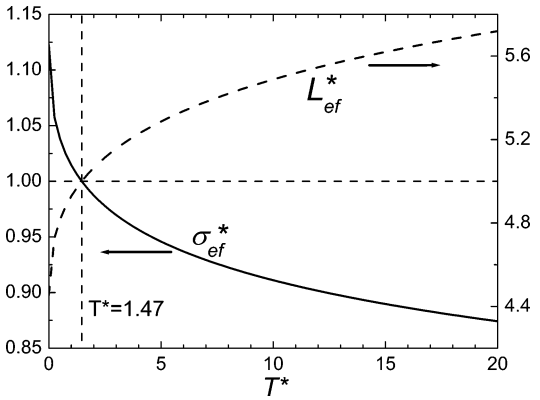

Figure 2. Effective hard spherocylinder molecular diameter, $\sigma^*_{ef} = \sigma_{ef}/\sigma$, assigned by eq 10 to the Kihara SRS potential as a function of the reduced temperature, $T^* = \kappa T/\epsilon$, and corresponding elongations of the effective HSC molecules, $L^*_{ef} = L/\sigma_{ef}$, for the case of the $L^* = L/\sigma = 5$ SRS fluid considered in this work.

$$\sigma_{ef} = \int_0^{\infty}(1 - \exp[-\beta U_{SRS}(d_m)])\, d(d_m) \quad (10)$$

The above integral is defined on the scalar d_m, the minimum distance between the central rods of the molecules. It is important to notice that eq 10 does not include any explicit dependence on the relative pair orientation nor, more remarkably, on the elongation of the molecules. Hence, this is one of the simplest means of performing the mapping between the soft and hard core models, which establishes a well-defined dependence of σ_{ef} on temperature but leaves out the effect of density or of the internal order of the liquid crystal phase on σ_{ef}, included in more refined treatments.[17,19,35] Despite this simplified approach, eq 10 will be shown to be sufficiently accurate for our purposes to describe the behavior of the SRS fluid in the vicinity of the isotropic−nematic transition. We note in passing that, since $U_{SRS}(d_m > d_{min}) \equiv 0$ (eq 1), the integrand of eq 10 vanishes for d_m values greater than $d_{min} = \sqrt[6]{2}\sigma$, which would be the split distance for a Kihara potential with repulsive and attractive interactions in the Weeks−Chandler−Andersen perturbation theory.[25]

Figure 2 depicts the temperature dependence of the effective molecular diameter $\sigma^*_{ef} = \sigma_{ef}/\sigma$ resulting from eq 10 for the temperature range scoped in this work. In the low temperature limit, the effective diameter tends to the maximum range of the SRS potential, $\sigma^*_{ef} \to \sqrt[6]{2}$, which simply means that at $T^* = 0$ the molecules are impenetrable. On the other hand, the value $\sigma^*_{ef} = 1.0$, for which the SRS and HSC fluids of the same diameter are expected to present similar properties within the present approximation, is achieved at a temperature of $T^* \approx 1.47$. Also worth noticing is the slow asymptotic decrease of σ^*_{ef} with growing temperature, due to the rapidly diverging repulsive wall of the SRS fluid at short distances (see Figure 1), so that $\sigma^*_{ef} \approx 0.87$ at $T^* = 20$, the highest temperature included in the present study.

Figure 2 shows as well that an interesting effect arises when the evolution with temperature of the effective elongation of the particles, $L^*_{ef} = L/\sigma_{ef}$, is considered. As can be observed, L^*_{ef} grows monotonically with temperature, and for the present case of the SRS fluid with $L^* = 5$, the elongation of the corresponding effective HSC fluid increases from $L^*_{ef} = 4.45$ at $T^* = 0$, through $L^*_{ef} = L^* = 5.00$ (i.e., equal to the elongation of the

TABLE 1: Parsons−Lee (P−L) and Monte Carlo (MC) Results for the Boundary States of the Isotropic−Nematic Transition in the SRS Fluid at the Isotherms Studied in This Work[a]

			P−L					MC				
T^*	σ^*_{ef}	L^*_{ef}	η_I	ρ^*_I	η_N	ρ^*_N	S_2	η_I	ρ^*_I	η_N	ρ^*_N	S_2
0.8	1.023	4.89	0.404	0.0866	0.423	0.0905	0.680	0.420(4)	0.090(1)	0.430(4)	0.092(1)	0.60(5)
1.0	1.015	4.93	0.402	0.0876	0.421	0.0917	0.680	0.413(4)	0.090(1)	0.427(4)	0.093(1)	0.54(3)
1.5	0.999	5.00	0.398	0.0897	0.417	0.0939	0.682	0.409(4)	0.092(1)	0.422(4)	0.095(1)	0.50(3)
2.0	0.987	5.06	0.396	0.0913	0.415	0.0957	0.683	0.403(4)	0.093(1)	0.416(4)	0.096(1)	0.52(3)
3.0	0.970	5.16	0.391	0.0938	0.410	0.0984	0.684	0.401(4)	0.096(1)	0.413(4)	0.099(1)	0.53(3)
5.0	0.946	5.29	0.385	0.0974	0.405	0.1023	0.686	0.396(4)	0.100(1)	0.408(4)	0.103(1)	0.55(3)
20.0	0.874	5.72	0.367	0.1095	0.387	0.1156	0.692	0.375(4)	0.112(1)	0.389(4)	0.116(1)	0.54(3)
HSC	1.000	5.00	0.399	0.0896	0.417	0.0938	0.688	0.407	0.0914	0.415	0.0932	0.47(5)

[a] The table indicates the densities, ρ^*_I and ρ^*_N, packing fractions, η_I and η_N, and nematic order parameters, S_2, of the boundary states. The packing fractions are calculated from the P−L and MC densities at each temperature as $\eta_{ef} = \rho v_{ef}$, where v_{ef} denotes the volume of the effective hard spherocylinder with the diameter, σ^*_{ef}, and elongation, L^*_{ef}, Values from eq 10 indicated in the table. Similar results for the HSC fluid[15] are also included for comparison.

HSC fluid with the same L) at $T^* = 1.47$, and up to $L^*_{ef} = 5.72$ at $T^* = 20$. This trend arises as an intrinsic property of the spherocylinder core geometry (e.g., for ellipsoidal particles, only the absolute size but not the effective aspect ratio would be affected by temperature) provided that a uniform pair interpenetration around the molecular core is assumed, and it will be shown (section 3) that it has a beneficial influence on the stability of the nematic phase and opposes the thermal "melting" of the long-range order.

D. Monte Carlo Simulations. Monte Carlo simulations in the isobaric−isothermal ensemble (MC-NPT) were run for the $L^* = 5$ SRS fluid at the same seven temperatures of the P−L study, $T^* = k_BT/\epsilon = 0.8$, 1.0, 1.5, 2.0, 3.0, 5.0, and 20.0. In addition, similar simulations were performed for the effective HSC fluids corresponding to those temperatures, with effective elongations of $L^*_{ef} = 4.89-5.72$ according to eq 10 (see Table 1). In each case, the simulations cover states of the isotropic (I) and nematic (N) phases and start from a high density nematic state which is subsequently expanded toward the low density limit through the nematic−isotropic transition. The phase transition is characterized by discontinuities in the density and the nematic order parameter as well as by sudden qualitative changes observed in specific orientation correlation functions.[15,21] No attempt was made for a more precise determination of the phase coexistence via thermodynamical integration or related techniques. On the other hand, the recompression of the fluid from the isotropic to the nematic state consistently led to negligible hysteresis effects for the I−N phase transition within the statistics of the MC simulations, which suggests that the boundary isotropic and nematic states in our simulations should be close enough for our purposes to the actual coexisting states.

The simulations were run over a system of $N_p = 768$ molecules. For some of the isotherms, the few states closest to the I−N transition were additionally simulated with twice the number of particles, $N_p = 1536$, to reduce finite size effects, and no appreciable differences were obtained. For a given state, after proper equilibration ($\sim 5 \times 10^5$ MC cycles) and ensemble averaging ($\sim 3 \times 10^5$ MC cycles), the last molecular arrangement was used as the initial configuration for the computation of the next state with a smaller system pressure. Each MC cycle consists of N_p trials for random displacements and/or reorientations of the particles, plus an attempt to change the box volume. The usual periodic boundary conditions were employed, and the box changes were performed with a fixed box geometry of $L_y/L_x = 1.15$ and $L_y/L_x = 1.94$. No changes in the results were observed in some test runs in which each of the box sides was varied independently, with the restriction that none of them became shorter than twice the range of the potential. Noticeably, despite this additional degree of freedom, the simulations typically kept average side ratios of $L_x \approx L_y < L_z$, similar to the ones imposed in the simulations with a fixed box geometry. The nematic director of the fluid aligned preferentially along one box diagonal.

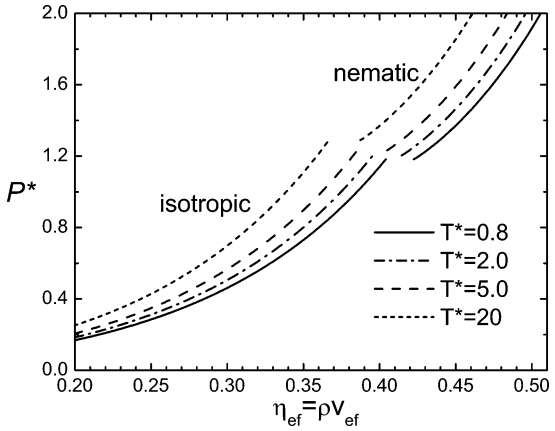

Figure 3. Parsons−Lee equations of state for the Kihara SRS fluid in the vicinity of the isotropic−nematic transition for some representative isotherms studied in this work. The P−L theory is solved for effective HSC systems with temperature-dependent diameters and elongations (see eq 10, Figure 2, and Table 1).

III. Results and Discussion

Figure 3 shows the equations of state (EOS) resulting from the P−L approximation for some of the isotherms of the SRS fluid explored in our work. The data are represented in a compact form by confronting pressure in the dimensionless reduced units $P^* = \beta P \sigma^3_{ef}$, with packing fraction $\eta_{ef} = \rho v_{ef}$, where $v_{ef} = \pi\sigma^3_{ef}/6 + \pi\sigma^2_{ef}L/4$ stands for the molecular volume of the effective hard spherocylinder representing the SRS molecules at each temperature.

As can be observed, at each temperature, the increase in the packing fraction of the system correlates, as expected, with a smooth but progressively more rapid increase of pressure. Conversely, at a fixed packing fraction, P^* also shows a systematic growth with increasing temperature. Note that, due to the use of temperature in the definition of P^*, this latter trend would actually become much more marked if pressure were considered in standard units, $P = P^*/\beta\sigma^3_{ef}$. The first-order character of the I−N transition is clearly appreciated in the isotherms of Figure 3 as a discontinuity in packing fraction that separates the isotropic and nematic branches. The inspection of the set of EOS shows that the transition pressure increases

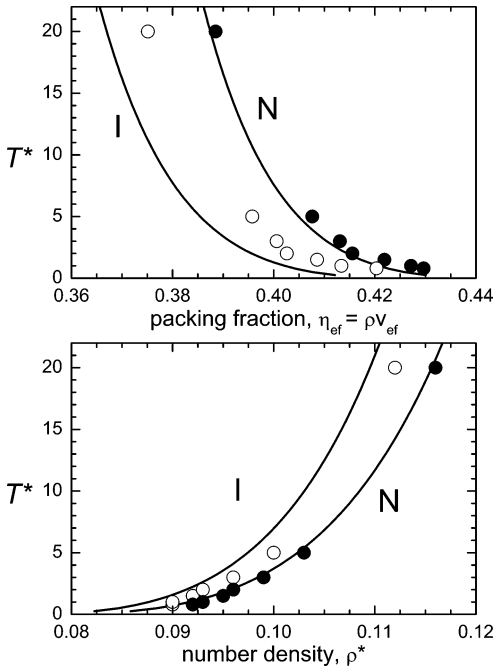

Figure 4. Effective packing fractions (top) and number densities (bottom) for the boundary states of the isotropic−nematic transition of the $L^* = 5$ SRS fluid within the range of temperatures covered in the present work, $T^* = 0.8-20.0$. The symbols denote MC-NPT simulation data, whereas the solid lines correspond to the prediction of the Parsons−Lee approach employed in this work. The effective packing fractions are obtained from the number densities with the molecular volume, v_{ef}, of the effective HSC fluids resulting from eq 10.

with growing temperature, and more interestingly, it reveals that the effective packing fractions of the isotropic−nematic coexistence decrease with temperature (see also Table 1). Hence, it appears that the nematic phase is stabilized relative to the isotropic phase by increasing the temperature. This effect seems contrary to the usual behavior observed with other rigid models (e.g., Gay−Berne fluid), and as will be shown, it arises as a consequence of the increase in the effective aspect ratio with temperature linked to the spherocylinder molecular geometry.

A more detailed insight into the behavior of the Kihara SRS fluid at the I−N transition is provided in Figure 4 and Table 1, which compare the isotropic and nematic coexistence branches predicted by the theory at the different temperatures scoped in our work with the boundary states obtained in the MC-NPT simulations. The qualitative and even quantitative agreement between both sets of data is remarkable given the gross approximations involved in the present Parsons−Lee approach. We first of all make notice of the fact that the P−L and MC results agree in a weak dependence of the nematic order parameter for the boundary nematic state of the I−N transition, although the Parsons−Lee order parameters, $S_2 = 0.68-0.69$, are systematically larger than those obtained in the MC simulations, $S_2 \approx 0.50-0.60$. Such differences for S_2 can be traced back to the fact that the $f(\theta)$ distributions resulting from the Parsons−Lee minimization procedure are narrower than those from the MC averaging. More importantly, the MC simulations corroborate the significant displacement of the I−N transition toward smaller effective packing fractions when heating the fluid (top panel of Figure 4). The SRS−HSC mapping model constitutes the heart of the definition of η_{ef} and can be invoked for a rationalization of this apparent stabilization of the nematic phase with growing temperature, which at first sight seems opposite to the expected thermal disordering of the fluid. In Figure 2, it was shown that the reduction of σ_{ef} with temperature also implies an increment of the effective elongation, L/σ_{ef}, of the spherocylinder molecules. A greater molecular elongation leads to an enhanced steric propensity that favors the entrance of the nematic phase (the system moves toward the Onsager limit). In fact, McGrother and co-workers[15] showed for the HSC fluid that increasing the elongation in the $L^* = 4-5$ range reduces significantly the packing fraction of the I−N transition. In this sense, Table 1 serves to illustrate that the temperature $T^* = 1.47$ divides the temperature scale into two regimes, as far as the comparison of the HSC and SRS fluids is concerned: for lower temperatures, $L^*_{ef} < L^*$, and for higher temperatures, $L^*_{ef} > L^*$. In fact, while there is good concordance for the coexistence data of the HSC fluid and the SRS fluid at $T^* = 1.5$ (which for the present discussion can be considered to represent the nominal $T^* = 1.47$), at lower temperatures, the I−N transition in the SRS fluid is delayed to greater effective packing fractions than that in the HSC fluid, meaning that steric effects (closely linked to molecular elongation) are less important in the latter case, whereas, on the contrary, for higher temperatures, the SRS I−N transition takes place at smaller packing fractions than in the HSC fluid, as a consequence of the increased effective molecular elongation. These results corroborate in a systematic way the predictions of an earlier work[21] based on the comparison of MC simulations of the SRS and HSC fluids with $L^* = 4$ and $L^* = 5$.

The lower panel of Figure 4 illustrates the behavior of the Kihara SRS fluid at the I−N transition in terms of the reduced number density, $\rho^* = \rho\sigma^3$. Note that, as opposed to the effective packing fractions, the transition densities do grow with temperature. This trend is consistent with the temperature dependence of the SRS−HSC mapping and can be used to provide an intuitive interpretation of the observed I−N coexistence as follows. The increase of temperature in the SRS fluid induces a progressively greater interpenetration of the particles which leads to a decrement of the effective size of the molecules and, consequently, to a loss of excluded volume. Hence, a gain in density is demanded in order to recover the packing fractions needed for nematic equilibrium. However, as a consequence of the greater effective molecular elongation at the higher temperatures, the molecules need to occupy a smaller average fraction of space before the nematic phase becomes stable with respect to the isotropic phase. The relevant aspect to our argumentation is that the increase of density required to stabilize the nematic phase is actually more moderate than would be expected considering that the heating of the fluid actually works in favor of a disordering of the fluid and, hence, of an *increase* of the transition packing fractions. Comparison of the two panels of Figure 4 indicates that thermal melting is more than compensated for by the stabilization of the nematic phase associated with the increase of L^*_{ef}.

It seems timely to proceed to provide a more detailed insight into the performance of the P−L approximation and the SRS−HSC mapping employed in our work by means of a comparison of the predicted equations of state with the result of Monte Carlo simulations. The determination of EOS for convex molecular fluids has been the object of numerous investigations.[27] Scaled particle theory constitutes a especially fruitful route in this context, yielding analytical expressions for the EOS in terms of molecular geometrical parameters, hence allowing for a rationalization of the behavior of the fluid with the language of pair and many-body excluded volume or macromolecular crowding. Remarkably, this is also the case for the Parsons−Lee approximation, which leads to the following expression for

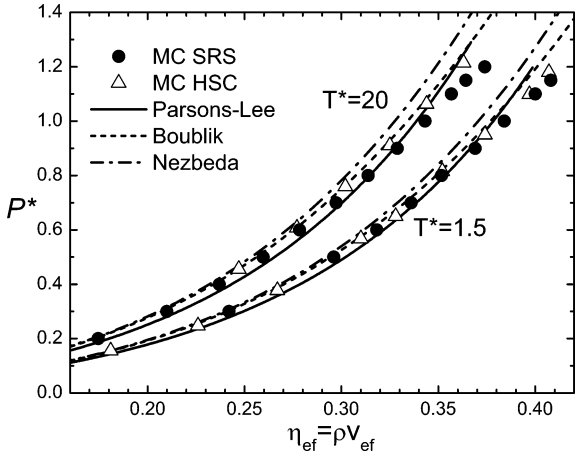

Figure 5. Comparison of the analytical equations of state given in eqs 11−13 with Monte Carlo simulation results for the isotropic phase of the SRS fluid (circles) at $T^* = 1.5$ and 20. Monte Carlo results are also shown for the effective HSC fluids (triangles) with the corresponding σ_{ef}^* and L_{ef}^* values from eq 10 (see Table 1).

the EOS in the isotropic phase:

$$Z = \frac{\beta P}{\rho} = 1 + \left(\frac{1+3\alpha}{4}\right)\frac{4\eta - 6\eta^2 + 2\eta^3}{(1-\eta)^4} \qquad (11)$$

where the molecular shape factor $\alpha = r_m s_m/(3v_m) = (L^* + 2)-(L^* + 1)/(3L^* + 2)$, extensively employed in the treatment of convex body fluids, is defined from the surface area, s_m, the mean curvature integral, $4\pi r_m$, and the volume, v_m, of the particles. It is worth pointing out that eq 11 can be obtained from the virial scaling approximation proposed by Vega and Lago.[43]

We will compare the P−L EOS with predictions from scaled particle theory, on one hand, with an early expression introduced by Nezbeda (eq 12)[44] and, on the other hand, with a recently refined form derived by Boublik (eq 13) from virial coefficients up to the fourth order:[45]

$$Z = \frac{1}{1-\eta} + \frac{3\alpha\eta}{(1-\eta)^2} + \frac{(\alpha^2 + 4\alpha - 2)\eta^2 - (5\alpha^2 - 4\alpha)\eta^3}{(1-\eta)^3} \qquad (12)$$

$$Z = \frac{1}{1-\eta} + \frac{3\alpha\eta}{(1-\eta)^2} + \frac{(3\alpha^2\xi)\eta^2 - (\alpha^3)\eta^3 - (\alpha^3 - 1)\eta^4}{(1-\eta)^3} \qquad (13)$$

where the additional parameter $\xi = [s_m/(4\pi r_m^2)]^{1/2}$ has been introduced in eq 13.

Figure 5 depicts the P−L EOS for the isotropic phase of the SRS fluid at two different temperatures, $T^* = 1.5$ and 20, together with the corresponding Monte Carlo results. In addition, the figure also includes the Monte Carlo data for the corresponding effective HSC fluids with $L_{ef}^* = 5.00$ ($\sigma_{ef}^* = 1.00$) and $L_{ef}^* = 5.72$ ($\sigma_{ef}^* = 0.87$), respectively, for comparison. The good overlap of the SRS and HSC data, closely followed in both cases by the Parsons−Lee EOS, provides confidence on the reliability of the simple mapping between both fluids employed in this work, meaning that the HSC fluid with the appropriate molecular breadth constitutes an effective zeroth-order representation of the SRS fluid in the isotropic phase. Figure 5 shows that the scaled particle expressions of Nezbeda and Boublik yield slightly greater pressures than the Parsons−Lee EOS but also reproduce accurately the MC results. In particular, the recent Boublik EOS provides a remarkable

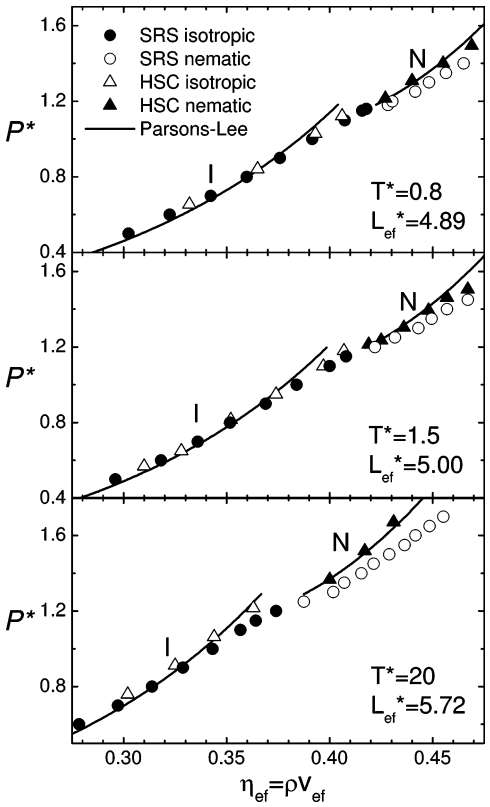

Figure 6. Comparison of the Monte Carlo (circles) and Parsons−Lee (solid curves) equations of state for the SRS fluid at three selected isotherms ($T^* = 1.5$, 5.0, and 20.0). The Monte Carlo results for the corresponding effective HSC fluids with the diameters and elongations, σ_{ef}^* and L_{ef}^* from eq 10 listed in Table 1, are also included in each panel (triangles).

agreement with the Monte Carlo data over the whole isotropic phase. The relative good agreement obtained with the 30-year-old EOS of Nezbeda for the high molecular elongations employed in our work is also worth noticing, especially at the smaller packing fractions ($\eta_{ef} < 0.3$). Further EOS from scaled particle theory proposed by Boublik[27] and by Barrio and Solana[46] for shorter molecules were tested, but none of them led to an improved agreement with the Monte Carlo results.

Figure 6 shows a full comparison between the Parsons−Lee and Monte Carlo EOS of the SRS fluid, including the isotropic and nematic phases. Three isotherms are chosen to illustrate the results, namely, $T^* = 0.8$, 1.5, and 20, to represent cases where $L_{ef}^* < L^*$ ($\sigma_{ef}^* > 1$), $L_{ef}^* \approx L^*$ ($\sigma_{ef}^* \approx 1$), and $L_{ef}^* > L^*$ ($\sigma_{ef}^* < 1$), respectively. The MC data for the corresponding effective HSC fluids are also included in each panel for comparison. Remarkable agreement is again found between the P−L and MC results for the SRS fluid throughout the isotropic phase up to the vicinity of the I−N transition at all temperatures. A systematic deviation of the Monte Carlo data from the theoretical predictions is only observed for the few isotropic states of greatest density. Although this may be attributed to a breakdown of the theoretical approximations, we could not rule out finite size effects in the MC simulations, even though no changes in the results were observed when a 2-fold increased number of particles was employed. For those states, located immediately before the entrance of the nematic phase, pretransitional fluctuations induce a weak but appreciable orientational order in the simulations, yielding nematic order parameters of up to $S_2 \approx 0.2$. This allows for a slightly more effective packing of the system at each pressure in comparison to the completely

disordered isotropic fluid, which may be responsible for the apparent greater densities with respect to the P−L EOS.

Within the nematic phase, whereas good qualitative agreement is found, the present P−L approach leads however to a systematic overestimation of the pressure (at a given packing fraction) of the SRS fluid, especially at the higher temperatures. On the other hand, Figure 6 shows that, when compared with the Monte Carlo simulations for the HSC fluid with the corresponding effective elongation, the P−L approximation actually performs remarkably well in both the isotropic and nematic phases. This result indicates that the Parsons−Lee scaling can actually be considered sufficiently accurate at the EOS level, which is noticeable considering the crude representation provided by the HS reference fluid, especially in the nematic phase, for the prolate HSC with molecular elongations as large as the ones considered in our work.

The apparent deviation of the P−L EOS from the MC data for the SRS fluid in the nematic phase may then be traced back to the additional approximation assumed in our work when representing the SRS fluid by an effective HSC fluid. Although the proposed mapping seems reasonable for the nematic SRS fluid at low temperatures (e.g., $T^* = 0.8$ and 1.5), where the MC SRS and HSC EOS almost overlap, it loses accuracy at higher temperatures. This result is not completely unexpected, since as the temperature increases the pair interactions sample a progressively broader range of pair contact distances, thereby making the average hard core contact distance representation of the HSC fluid less accurate.

IV. Summary and Conclusions

The Parsons−Lee theory and Monte Carlo simulations have been employed to investigate the behavior of soft repulsive prolate molecular fluids in the vicinity of the isotropic−nematic transition over a broad temperature range. To solve the P−L equations, a simple mapping introduced in previous works has been employed to represent the soft interaction potential by an effective hard core interaction with a temperature-dependent molecular diameter meant to represent the average thermal size of the soft molecules.

The methodology is general, and for the present work, it has been applied to the particular case of the repulsive Kihara SRS fluid. The spherocylinder molecular geometry of the SRS fluid has the peculiarity of imposing an effective increase of the elongation of the molecules with temperature in an implicit way to the reduction of the effective molecular diameter associated with the greater short-distance interpenetration of the molecular pairs. Our results show that this shape effect competes favorably with the expected thermal disordering of the fluid and induces a stabilization of the nematic phase at smaller effective packing fractions, contrary to what is found with fluid models of different symmetries (e.g., ellipsoidal).

The observed effect can be rationalized in terms of excluded volume arguments. The heating of the SRS fluid reduces the effective size of the molecules, and a gain in density is required in order to recover the steric constraints needed for nematic equilibrium. However, as a consequence of the greater effective molecular elongation at the higher temperatures, the molecules require a substantially smaller packing fraction before the nematic phase becomes stable with respect to the isotropic phase. The consequence is that the densities required to stabilize the nematic phase are actually smaller than expected, especially taking into account that, contrary to our findings, the thermal melting trend associated with the heating of the fluid would be expected to lead to an increase of the transition packing fractions.

Overall, a remarkable general agreement is found between the Parsons−Lee approach and the Monte Carlo simulations for the equation of state of the fluid, including the isotropic−nematic phase boundaries. Such a level of agreement was not necessarily expected, considering the gross approximations involved, on one hand, in the P−L theory and, on the other hand, in the simple mapping between the SRS and HSC fluids employed. For the molecular elongations considered in the present work, the theoretical approach provides a more accurate EOS in the isotropic phase of the fluid than any of the analytical expressions proposed in the past, mainly based on scaled particle theory.

The performance of the methodology in the nematic phase of the SRS fluid is fair but less accurate than that in the isotropic phase, especially in the high temperature regime where it leads to a systematic overestimation of the pressure at a given fluid density (or, conversely, to an underestimation of the equilibrium density at a given pressure). Interestingly, the P−L theory as employed here does perform quite well when compared with the simulation results for the EOS of the effective HSC fluid corresponding to each temperature. This result is noticeable, taking into account the relatively large molecular elongations considered and the simplicity of the Parsons−Lee scaling employed, in which the HS fluid is taken as a reference system in both the isotropic and nematic phases.

The quantitative discrepancies between the theoretical predictions and the MC simulations for the nematic phase of the SRS fluid must therefore be attributed to an oversimplification of the treatment of the steric effects in the mapping employed between this fluid and the HSC system in order to solve the P−L equations, especially at the higher temperatures for which a broader range of effective contact distances are involved in the pair interactions. The main limitations of the present SRS−HSC mapping are presumably related to the lack of dependence of the effective molecular size on density and on the liquid crystal phase of the fluid, as considered in previous works for colloidal systems.[17,19,35]

Despite the limitations mentioned above, the qualitative and even quantitative accuracy of the present treatment is remarkable, and it should be useful in different contexts in which soft interacting particles are relevant. In particular, the same methodology could be applied to make predictions for charged colloids where environmental parameters such as ionic strength play a similar role as temperature in controlling the range of the pair interactions and hence the effective size of the molecules. Since the spherocylinder geometry is expected to provide a reliable coarse-grained representation of real fluids of elongated bodies, the concept of an environment-dependent molecular elongation must be borne in mind when making predictions about the steric and mesogenic behavior of these types of fluids.

Acknowledgment. We thank G. Jackson (Imperial College, London) for wise comments on the results presented in this work. Financial support is acknowledged from the Ministry of Education and Science of Spain (grants CTQ2004-07730-C02 and VEM2003-20574-C03) and from the Regional Government of Andalusia (groups PAI FQM-205 and FQM-319).

References and Notes

(1) Tarazona, P. *Philos. Trans. R. Soc. London, Ser. A* **1993**, *344*, 307.
(2) Onsager, L. *Ann. N. Y. Acad. Sci.* **1949**, *51*, 627.
(3) Maier, W.; Saupe, A. *Z. Naturforsch.* **1958**, *13a*, 564; **1960**, *15a*, 287.
(4) Somoza, A. M.; Tarazona, P. *Mol. Phys.* **1992**, *75*, 17.

(5) Wulf A. *J. Chem. Phys.* **1977**, *67*, 2254.
(6) Parsons, J. D. *Phys. Rev. A* **1979**, *19*, 1225.
(7) Lee, S. D. *J. Chem. Phys.* **1987**, *87*, 4972.
(8) Baus, M.; Colot, J. L.; Wu, X. G.; Xu, M. *Phys. Rev. Lett.* **1987**, *59*, 2184.
(9) Somoza, A. M.; Tarazona, P. *Phys. Rev. A* **1990**, *41*, 965.
(10) Velasco, E.; Mederos, L.; Sullivan, D. E. *Phys. Rev. E* **2000**, *62*, 3708.
(11) Galindo, A.; Haslam, A. J.; Varga, S.; Jackson, G.; Vanakaras, A. G.; Photinos, D. J.; Dunmur, D. A. *J. Chem. Phys.* **2003**, *119*, 5216.
(12) Cinacchi, G.; Mederos, L.; Velasco, E. *J. Chem. Phys.* **2004**, *121*, 3854 and references therein.
(13) Cuetos, A. Ph.D. Thesis, Universidad Pablo de Olavide, Seville, Spain, 2004. Cuetos, A. *Fases fluidas ordenadas mediante modelos moleculares rıgidos con potenciales de interacción sencillos*; Anavia Ed.: Seville, Spain, 2005; ISBN 84-934302-0-X.
(14) Vroege, G. J.; Lekkerkerker, H. N. W. *Rep. Prog. Phys.* **1992**, *55*, 1241.
(15) McGrother, S. C.; Williamson, D. C.; Jackson, G. *J. Chem. Phys.* **1996**, *104*, 6755.
(16) Bolhuis, P.; Frenkel, D. *J. Chem. Phys.* **1997**, *106*, 666.
(17) Kramer, E. M.; Herzfeld, J. *J. Chem. Phys.* **1999**, *110*, 8825.
(18) Kramer, E. M.; Herzfeld, J. *Phys. Rev. E* **2000**, *61*, 6872.
(19) Graft, H.; Löwen, H. *Phys. Rev. E* **1999**, *59*, 1932.
(20) Holyst, R.; Ostwald, P. *Macromol. Theory Simul.* **2001**, *10*, 1.
(21) Cuetos, A.; Martınez-Haya, B.; Rull, L. F.; Lago, S. *J. Chem. Phys.* **2002**, *117*, 2934; **2002**, *117*, 11405 (erratum).
(22) Martınez-Haya, B.; Cuetos, A.; Lago, S.; Rull, L. F. *J. Chem. Phys.* **2005**, *122*, 024908.
(23) Frenkel, D.; Mulder, B. M.; McTague, J. P. *Phys. Rev. Lett.* **1984**, *52*, 287.
(24) Barker, J. A.; Henderson, D. *J. Chem. Phys.* **1967**, *47*, 4714. Henderson, D.; Barker, J. A. *J. Chem. Phys.* **1970**, *52*, 2315.
(25) Weeks, J. D.; Chandler, D.; Andersen, H. C. *J. Chem. Phys.* **1971**, *54*, 5237.
(26) Boublik, T. *J. Chem. Phys.* **1987**, *87*, 1751.
(27) Boublik, T. In *Equations of State for Fluids and Fluid Mixtures, part I*; Sengers, J. V., Kaiser, R. F., Peters, C. J., White, H. J., Jr., Eds.; Elsevier: Amsterdam, The Netherlands, 2000.
(28) Padilla, P.; Lago, S. *Fluid Phase Equilib.* **1989**, *48*, 53.
(29) Vega, C.; Lago, S.; Padilla, P. *J. Phys. Chem.* **1992**, *96*, 1900.
(30) Adams, M.; Dogic, Z.; Keller, S. L.; Fraden, S. *Nature* **1998**, *393*, 349.
(31) Kihara, T. *Adv. Chem. Phys.* **1963**, *5*, 147.
(32) Cuetos, A.; Martınez-Haya, B.; Lago, S.; Rull, L. F. *Phys. Rev. E* **2003**, *68*, 011704.
(33) Aoki, K. M.; Akiyama, T. *Mol. Simul.* **1996**, *16*, 99. Aoki, K. M.; Akiyama, T. *Mol. Cryst. Liq. Cryst.* **1997**, *299*, 45.
(34) Earl, D. J.; Ilnytskyi, J.; Wilson, M. *Mol. Phys.* **2001**, *99*, 1719.
(35) Stroobants, A.; Lekkerkerker, H. N. W.; Frenkel, D. *Phys. Rev. Lett.* **1986**, *57*, 1452. Stroobants, A.; Lekkerkerker, H. N. W.; Odijk, Th. *Macromolecules* **1986**, *19*, 2232.
(36) Vega, C.; Lago, S. *Comput. Chem.* **1994**, *18*, 55.
(37) Lakatos, K. *J. Stat. Phys.* **1970**, *2*, 121.
(38) Lasher, G. *J. Chem. Phys.* **1970**, *53*, 4141.
(39) Kayser, R. F.; Ravaché, H. J. *Phys. Rev. A* **1978**, *17*, 2067.
(40) Lekkerkerker, H. N. W.; Coulon, P.; van der Haegen, R.; Deblieck, R. *J. Chem. Phys.* **1984**, *89*, 3427.
(41) Boublik, T.; Nezbeda, I. *Collect. Czech. Chem. Commun.* **1986**, *51*, 2301.
(42) Boublik, T. *Mol. Phys.* **1981**, *42*, 209.
(43) Vega, C.; Lago, S. *J. Chem. Phys.* **1994**, *100*, 6727.
(44) Nezbeda, I. *Chem. Phys. Lett.* **1976**, *41*, 55.
(45) Boublik, T. *J. Phys. Chem. B* **2004**, *108*, 7424.
(46) Barrio, C.; Solana, J. R. *Mol. Phys.* **1998**, *94*, 809.